KNMI Climate Explorer: A web-based research tool for high-resolution paleoclimatology

RESEARCH TOOLS

KNMI CLIMATE EXPLORER: A WEB-BASED RESEARCH TOOL FOR HIGH-RESOLUTION PALEOCLIMATOLOGY

VALERIE TROUET[1] and **GEERT JAN VAN OLDENBORGH**[2]*

[1]Laboratory of Tree-Ring Research, University of Arizona, Tucson, AZ, 85721, USA

[2]Royal Netherlands Meteorological Institute KNMI, P.O. Box 201, NL-3730 AE De Bilt, Netherlands

ABSTRACT

Climate Explorer (www.climexp.knmi.nl) is a web-based application for climatic research that is managed by the Royal Netherlands Meteorological Institute (KNMI) and contains a comprehensive collection of climatic data sets and analysis tools. One of its fields of application is high-resolution paleoclimatology. We show how Climate Explorer can be used to explore and download available instrumental climate data and derived time series, to examine the climatic signal in uploaded high-resolution paleoclimate time series, and to investigate the temporal and spatial characteristics of climate reconstructions. We further demonstrate the value of Climate Explorer for high-resolution paleoclimate research using a dendroclimatic data set from the High Atlas Mountains in Morocco.

Keywords: KNMI Climate Explorer, paleoclimatology, dendroclimatology, time-series analysis, climate data, composite analysis, correlation map, spectral analysis.

INTRODUCTION

Since 1999, the Royal Netherlands Meteorological Institute KNMI has been managing and updating the Climate Explorer (climexp.knmi.nl), a web-based application for climatic research that contains a comprehensive collection of climatic data sets and analysis tools. After free registration, researchers can explore and download an array of climatic data sets, generate derived data, upload their own time series, and run statistical analyses to investigate and compare data sets. The KNMI Climate Explorer (hereafter referred to as CE) was originally intended for ENSO teleconnection analysis (van Oldenborgh and Burgers 2005). It has rapidly grown to become a useful tool for other climate research fields such as climate change research (van Oldenborgh *et al.* 2009) and the paleoclimate research community currently forms one of its largest user communities (*e.g.* Abram *et al.* 2008; Camuffo *et al.* 2010; Poljansek *et al.* 2012). Its primary uses for high-resolution

paleoclimatology include (1) exploring and downloading available instrumental climate data and derived time series, (2) examining the climatic signal in uploaded high-resolution paleoclimate time series, and (3) investigating the temporal and spatial characteristics of climate reconstructions.

In this note, we demonstrate the above-mentioned uses of CE for dendroclimatic analysis, but the techniques can easily be extrapolated to other high-resolution paleoclimatic data sets (*e.g.* coral data and varved sediments). A PDF document that includes a step-by-step instruction manual organized according to the same structure as the main text is available from the journal website as Supplementary Material. We restrict our demonstration to a dendroclimatic data set, but it will become clear that several applications are also useful for other dendrochronological fields, particularly event-based dendro-ecology (*e.g.* Trouet *et al.* 2010). It is worth mentioning that CE supports a comprehensive help overview (http://climexp.knmi.nl/help.cgi) that can be consulted for additional information. Throughout this paper, we use an Atlas cedar (*Cedrus atlantica*)

*Corresponding author: oldenborgh@knmi.nl

tree-ring width (TRW) chronology from Jaffa (JAF) in the High Atlas Mountains in Morocco (Esper *et al.* 2007) as an example of a dendroclimatic data set. The chronology is based on 52 tree-ring series from 32 trees that cross-correlate significantly (average cross-correlation r-value = 0.83) and cover the period A.D. 1021–2001. For the purpose of this exercise, the individual contributing series were detrended using a negative exponential curve of any slope to remove growth trends (Fritts 1976).

EXPLORATION OF INSTRUMENTAL DATA SETS

CE provides a plethora of instrumental climate data sets in the form of either time series (station data and climate indices) or gridded fields (observations and reanalysis fields). All data sets can be accessed and investigated by selecting the appropriate time series or fields format on the CE web page. For dendroclimatic analysis, monthly time series and fields are most useful, and we will therefore focus on the monthly data sets. Note, however, that specific daily climate data can easily be transformed to monthly and lower resolution in CE. The search for available instrumental data for a certain location (*e.g.* a tree-ring site) can be approached in two ways by selecting (1) station data or (2) gridpoint data. When a time series or derived time series (see below) of either kind is selected, it is important to make it available for further analysis by adding it to the list of user-defined time series.

Selection of Available Station Data for a Site

Amongst other databases, CE provides access to two NOAA/NCDC Global Historical Climatology Network monthly (GHCN-M) v2 databases of adjusted and unadjusted monthly station data (Diamond and Lief 2009). Both data sets contain monthly precipitation and mean temperature data that are valuable for dendroclimatic analysis. The adjusted set is corrected for urban effects and other biases and is generally preferable, but its availability is limited in time, space, and variable. Comparing the outcome of both data set

selections is therefore recommended. It is worth noting that monthly or daily time series of other climatic variables are also available, which can be useful for dendroclimatic and dendrohydrological research, including river discharge (Woodhouse *et al.* 2006), cloud cover (Young *et al.* 2010), and snow depth (Pederson *et al.* 2011).

When selecting a time series of monthly station data, the researcher is given the opportunity to make a selection based on station name (if the station of interest is known) or on vicinity to a location. The second option includes searching for a defined number of stations nearest to a given site or all stations within a defined region. Furthermore, a minimum number of years of data availability can be defined as well as a range of years for which data should be available and an elevation range. As an example, we searched for the five stations nearest to JAF (32°32′N 4°55′W; 2200 m a.s.l.) and applied a filter of a minimum of 30 years of monthly data availability. No adjusted GHCN precipitation data are available for Morocco or its neighboring countries (the nearest station is in Chimay, Belgium, 49.98°N 4.35°E). For further analysis, we thus selected the non-adjusted station with the longest available time series (Meknes; 33.90°N 5.50°W, 549 m a.s.l.; 1931–2011). In general, researchers will take length of time series, proximity to site, and elevation into account when selecting (a) station(s) for dendroclimatic analyses, as well as availability of various climatic variables. Selection is likely to be more complex for precipitation data than for temperature data because of the strong localized effects on interannual precipitation variability that arise from orography and other physical processes, *versus* more broad patterns in interannual temperature variability (Büntgen *et al.* 2010).

Upon selecting a station, the researcher is offered three plots of the absolute value time series, the annual cycle of the climatic variable at this site, and the time series of anomalies with respect to this annual cycle. Furthermore, the selected time series can be high- and low-pass filtered: high-pass filtering eliminates the influence of low-frequency variability and trends when calculating cross-correlations, whereas low-pass filtering can be of use when working with non-annually resolved

paleoclimate data. Also lower resolution (monthly, seasonal, and annual) time series of average, maximum, or minimum values can be derived from the selected data series. Using this function, threshold-delimited time series can be created that represent the sum above or below or the number of values that reach a defined threshold. If daily data are available for a site, this function can be used to calculate monthly number of growing degree days by creating a monthly time series of the number of days with a mean temperature greater than 10°C.

Selection of Gridpoint Data

For regions where publicly available station data are few or far between, gridpoint data can provide a valuable alternative. An added advantage of gridpoint data is that long time series are available for many climate variables. These datasets come in three flavors: analyses, reconstructions, and reanalyses. An analysis (*e.g.* the HADCRU observational surface temperature data sets; Jones 1994; Jones and Moberg 2003; Brohan *et al.* 2006; Morice *et al.* 2012) is simply an interpolation of all available data, which often includes non-public time series that are not available for download. Areas and times without data are left blank. A reconstruction (*e.g.* the GISS surface temperature data sets, Hansen *et al.* 1981; Hansen and Lebedeff 1987; Hansen *et al.* 2010) functions in the same way, except that data gaps are filled to the maximum extent possible. These gridpoints/time steps often do not contain useful information and should be avoided. A reanalysis (*e.g.* the NCAR/NCEP reanalysis data set, Kalnay *et al.* 1996) uses a weather model to interpolate between the observations, which is the optimal way to propagate information to data-sparse areas. However, this power comes at the expense of model biases and inhomogeneities at the time when new data sources become available (*e.g.* satellite data in the late 1970s).

For dendroclimatology, the CRU TS3.10 data set of monthly gridded (0.5°, 1°, and 2.5°) fields, developed by the Climate Research Unit of the University of East Anglia (Mitchell and Jones 2005) is of particular interest because of its global coverage, its long temporal extent (1901–2009),

and its abundance of climatic variables. These variables include the self-calibrating Palmer Drought Severity Index (scPDSI, Wells *et al.* 2004), a variant on the original PDSI drought index (Palmer 1965) that incorporates lagged time series of precipitation and temperature, as well as soil characteristics, is comparable for different climate regimes, and is a useful drought metric in regions where drought rather than temperature is the limiting factor for tree growth (*e.g.* Cook *et al.* 2004). A data set comparable in spatial and temporal resolution and extent to the CRU TS3.10 data set, but including precipitation data only, is produced by the Global Precipitation Climatology Centre (GPCC; http://gpcc.dwd.de) and provides gridded monthly precipitation sets based on data from *ca.* 64,400 stations.

Additional climate variables, including sea level pressure (SLP), geopotential height fields at various elevations, and a variety of derived variables (*e.g.* wind speed and relative humidity), are available in the NCAR/NCEP Reanalysis data set (Kalnay *et al.* 1996), which offers a 2° global grid of modeled monthly variables. Because of its relatively long time series (1948-present), this data set is valuable for dendroclimatology and particularly for the analysis of atmospheric circulation patterns (*e.g.* a reconstruction of the Pacific North American (PNA) pattern in Trouet and Taylor 2010; see also sections 2 and 3). However, it should be kept in mind that the weather model used to produce this reanalysis is of mid-1990s vintage and has some large biases, particularly in surface air temperature and precipitation (Kistler *et al.* 2001; Harnik and Chang 2003; Sturaro 2003; Bromwich and Fogt 2004). Recently, the Twentieth Century Reanalysis data set (Compo *et al.* 2011) has been uploaded to CE, which covers the same variables over even longer time-scales (1878–2010).

Note that a large range of gridded data sets is available in CE, which are not explicitly mentioned here. The aim of a study and the role of gridded data sets in this study will determine which data set should best be used. It is therefore recommended to read the information links available for all data sets before making a decision. These links also provide the necessary citations for all data sets.

Upon selection of a field, the researcher is given the choice to retrieve data for a single gridpoint or for an area. Similar options to derive high- and low-pass filtered and lower resolution time series are provided for gridpoint data as previously described for station data. Differences in the intra- and inter-annual precipitation variability for three potential instrumental precipitation data sets for the JAF chronology are shown in Figure 1. The three data sets include precipitation data from the Meknes station data and the nearest gridpoint data from the CRU TS3.0 (0.5°) and GPCC (0.5°) databases. The intra- and interannual comparisons demonstrate that the GPCC data for this location generally have lower values than the two other data sets, which reflect comparable absolute amounts of precipitation. The Meknes station data on the other hand has a shorter time-series length than the other two data sets and includes a substantial amount of missing data from 1984 onwards. Taking these factors into account, the CRU TS3.0 data set appears to be the most reliable record for calibration of the JAF chronology.

EXAMINATION OF THE CLIMATE SIGNAL IN DENDROCLIMATIC TIME SERIES

Uploading a Tree-Ring Series

CE is a powerful tool for initial and exploratory examination of dendroclimatic time series. It allows uploading of a user-defined time series and running a variety of statistical analyses. Uploaded time series will remain accessible in CE for three days after last use. After uploading, a plot of the data can be viewed, as well as a plot of the anomalies with respect to the average over a defined range of years.

When uploading a dendroclimatic time series, it is important to be aware that CE only correlates data sets with the same temporal resolution (*i.e.* monthly with monthly, annual with annual). Therefore, uploaded and existing data sets should be converted to the same resolution. To correlate an annually-resolved tree-ring series with annual instrumental climate data, an annually-resolved climate time series can be derived from monthly (or daily) data as described above. When a comparison of tree-ring data with monthly climate data (*e.g.* for
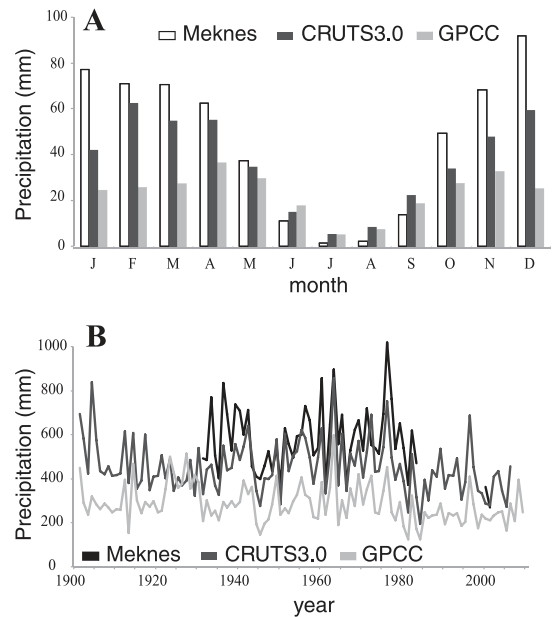

Figure 1. Precipitation climatology (A) and interannual annual (Jan–Dec) precipitation variability (B) for three instrumental data sets in the vicinity of Jaffa, Morocco (32.53°N, 4.9°W). The data sets include the Meknes meteorological station (33.90N, 5.50W) and gridpoint data from the CRUTS3.0 and GPCC (0.5°; 33°N, 5°W) databases.

response function analysis) is desired, the tree-ring series should be converted to monthly resolution. An annual or seasonal time series can be uploaded and reduced to monthly resolution in CE, which also allows for a choice of which months the signal is most representative. An alternative (and likely more straightforward) method for calculating seasonal comparisons is described in the next subsection. It is worth noting that "downscaling" an annual tree-ring time series to monthly or seasonal resolution, as described above, can redden the spectrum of the time series and can thus introduce artifacts in the spectral properties (see next section) of the downscaled time series (Schulz and Stattegger 1997; Schulz and Mudelsee 2002).

Correlation of Tree-Ring Time Series with Other Time Series

CE allows the user to correlate an uploaded time series with other user-defined time series as well as with system-defined time series (including various climate indices) of the same temporal

resolution. We comment on the investigation of monthly-resolved dendroclimatic time series, but analyses of seasonally and annually resolved series are comparable.

Analysis options include (rank) correlation or (least-square) regression analysis (Press *et al.* 1992, Ch. 14, 15) for individual or all months of the calendar year (January-December). The user is also given the option to calculate correlation coefficients using the average of multiple months of climate data. Furthermore, there is the option of calculating lagged correlations, which allows for the investigation of the influence of climatic conditions during the previous year on current year growth. Positive lags represent the tree-ring series lagging the climate data by a defined number of months. Given the difference in growth year for the tree-ring data (roughly April-September for the NH) and calendar year for the climate data (January-December), caution is warranted when interpreting the generated results. It is often best to investigate one lag and season separately to verify that the months (shown on the axes of the scatter plot) are correct.

All results are accompanied by estimates of the significance in the form of a *p*-value for a two-sided t-test assuming the underlying data are normally distributed (Press *et al.* 1992, Ch. 14). A 95% confidence interval on the correlation or regression coefficient is computed using a non-parametric bootstrap (Efron and Tibshirani 1998). If the data have been low-pass filtered prior to the correlation step, the user has to specify the decorrelation length (*i.e.* the cut-off length of the applied filter) explicitly for the computation of the significance and error bounds.

Other selection options include a range of years over which the correlation is run and upper and lower thresholds for both tree-ring and climate data. Selecting one or several threshold values restricts the range of values considered for correlation. Furthermore, running correlation and regression analyses can be performed with a user-defined time-window and the significance of running correlations can be tested with a Monte Carlo test (Gershunov 2001). CE also offers the opportunity to detrend the tree-ring and climatic series, but the detrending filters offered are generally too coarse for dendroclimatic analysis and we recommend detrending the tree-ring series using dendro-specific software (*e.g.* ARSTAN, Cook 1985) before uploading in CE.

Correlation analysis and regression analysis require a normal variable distribution. When variables are not normally distributed (*e.g.* snow-pack, fire occurrence, insect outbreaks), applying a logarithmic or square root transformation to the variable can bring the distribution closer to normal and improve the results. Another option is to compute rank correlation coefficients (Press *et al*. 1992) that do not make assumptions about the underlying distribution. Finally, CE provides the option to fit non-linear (parabolic, cubic) functions to the tree-ring time series.

Field Correlations

Time series uploaded in CE can be not only compared to other time series, but also to gridded fields of observational and reanalysis climate data. These field analyses typically result in correlation, regression, or composite maps (Von Storch and Zwiers 2002; Mudelsee 2010) that can be used for data exploration, but also to examine the spatial extent of the climatic signal present in a tree-ring series (Treydte *et al.* 2007; Fan *et al.* 2009; Büntgen *et al.* 2010) and to investigate teleconnection patterns (Buckley *et al.* 2007; D'Arrigo *et al.* 2008; Trouet *et al.* 2012). Correlation maps for SLP and geopotential height fields are particularly useful in the analysis of atmospheric circulation patterns (Trouet *et al.* 2009; Trouet and Taylor 2010; Baker *et al.* 2011; D'Arrigo *et al.* 2011).

Once the appropriate field is selected, the options for field correlation analysis are comparable to those for the time-series correlation analysis as described in the previous subsection. Additional options refer to the map output: the CE user can select map projection, boundaries, and color scale and can define contours and significance levels to be shown/masked out. The resulting maps can be saved as pdf or eps files or can be output as kml files for use in Google Earth or as GeoTIFF files for GIS software. For computational efficiency, the levels of significance are computed using a two-sided t-test, taking serial
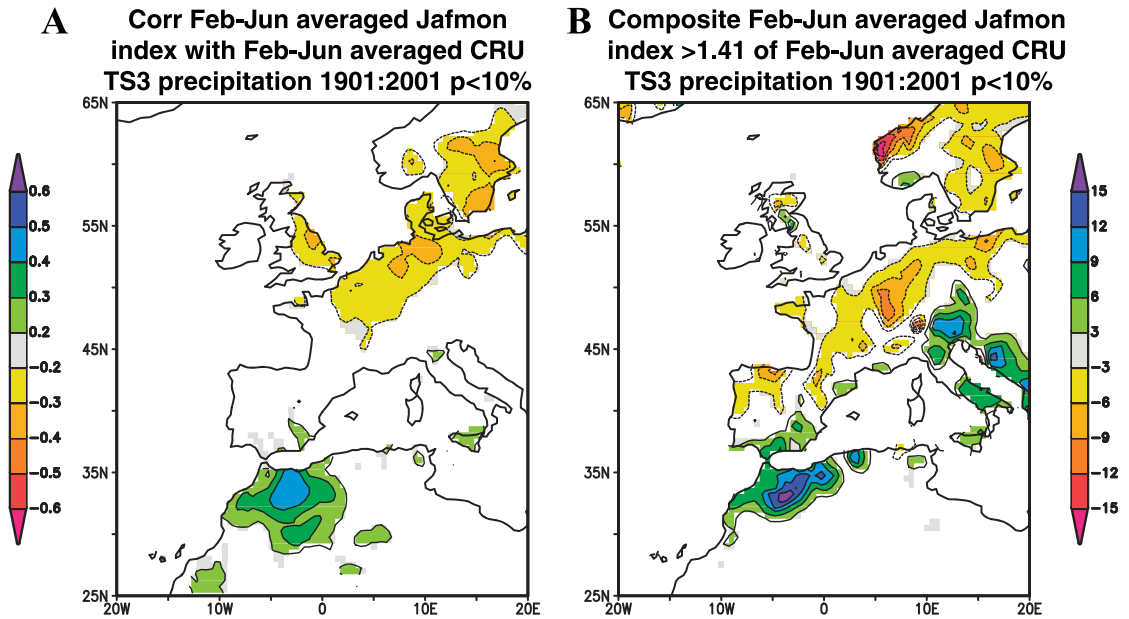
A **Corr Feb-Jun averaged Jafmon index with Feb-Jun averaged CRU TS3 precipitation 1901:2001 p<10%**

B **Composite Feb-Jun averaged Jafmon index >1.41 of Feb-Jun averaged CRU TS3 precipitation 1901:2001 p<10%**

Figure 2. Correlation (A) and composite (B) maps for the JAF tree-ring chronology with February–June CRUTS3.0 gridded (0.5°) precipitation fields (1901–2001). Composite maps are calculated for the 90th percentile of the JAF chronology over the period 1901–2001 (*i.e.* 10 years with highest TRW value). Colored contours represent significant correlation coefficients in A and significant anomalies from the 1901–2001 average in B.

correlations into account wherever these are statistically significant at $p < 0.05$. Again, if the data are not normally distributed and cannot be mapped into a normal distribution using a logarithm or square root, a rank correlation can be computed instead. Finally, it should be kept in mind that even in the absence of a real physical mechanism, generated maps will on average show 10% of the area colored with correlations with $p < 0.1$ because of random fluctuations. CE estimates roughly whether the area on the map is significantly larger than expected by pure chance and gives an indication of this 'field significance'. Interpretation of correlation maps also depends strongly on the physics: a small area at the expected position is more likely a true signal than a large area at the other side of the globe.

Another important additional option is the ability to create composite maps (*e.g.* Hastenrath 1976, 1978; Ropelewski and Halpert 1987; Galarneau *et al.* 2010). In composite map analysis, climatic field variables are averaged over selected years and the significance of the difference between this average and the average of the variable over the full time series is estimated and indicated on the resulting map (non-significant fields are masked out by default). A comparison of correlation and composite maps for the JAF tree-ring chronology with gridded precipitation fields (Figure 2) demonstrates that composite maps for continuous, normally distributed time series (most dendroclimatic series) will largely resemble correlation maps, albeit with more noise (less statistical power). The composite map approach is more appropriate for non-continuous, event-based time series (*e.g.* wildfire activity reconstruction in Trouet *et al.* 2010), for continuous time series that are not normally distributed, or when a nonlinear relationship is suspected.

DENDROCLIMATIC TIME-SERIES ANALYSIS

CE includes a number of gridded climate fields reconstructed from proxy and historical climate data that include seasonal temperature (A.D. 1500–2002; Luterbacher *et al.* 2004; Xoplaki *et al.* 2005), precipitation (A.D. 1500–2000;
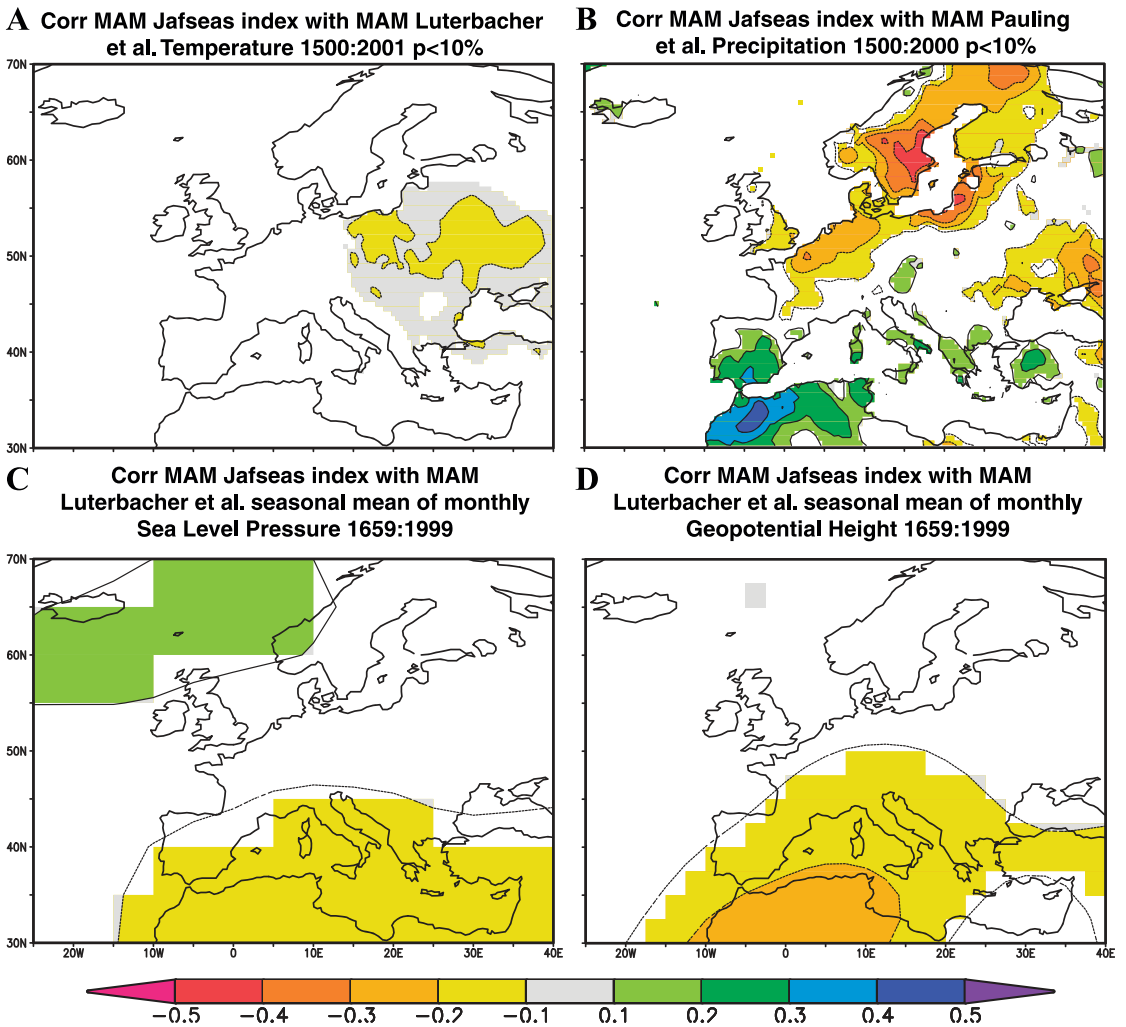
Figure 3. Correlation maps for the JAF tree-ring chronology with reconstructed (March–May) fields of (A) temperature (A.D. 1500–2001; Luterbacher *et al.* 2004); (B) precipitation (1500–2000; Pauling *et al.* 2006), (C) SLP (1659–1999; Luterbacher *et al.* 2002), and (D) 500 hPa geopotential height (1658–1999; Luterbacher *et al.* 2002). Only weak correlations are found with eastern European temperature fields, but the precipitation field shows a consistent pattern of positive correlation with precipitation over the Western Mediterranean and negative correlations over northwestern Europe. Circulation reconstructions (SLP and 500 hPa geopotential height) show weak but significant signals over northwest Africa. The precipitation correlation map (B) furthermore shows a strong resemblance with the correlation map for instrumental precipitation fields (Figure 2A). Statistically significant (p < 0.1) correlations with absolute values lower than 0.1 are indicated by grey shading.

Pauling *et al.* 2006), sea level pressure (SLP; A.D. 1750–2008; Luterbacher *et al.* 2002; Kuttel *et al.* 2010), and 500 hPa geopotential height (A.D. 1658–1999; Luterbacher *et al.* 2002) for Europe, summer temperature and SLP (A.D. 1600–1877; Briffa *et al.* 2002) for the circum-Arctic, and summer PDSI for the contiguous U.S.A. (A.D. 1000–2003; Cook *et al.* 2004) and for Monsoon Asia (A.D. 1300–2005; Cook *et al.* 2010).

Comparing uploaded tree-ring series to these reconstructed climate fields allows for the development of correlation, regression, and composite maps with similar options as described above (Figure 3).

To complete the spatiotemporal analysis of climate reconstructions, CE provides the opportunity to perform simple spectral, autocorrelation, and wavelet analysis. CE can be used to compute

the autocorrelation function $a_n = \langle X_i X_{i+n} \rangle / \langle X_i X_i \rangle$ and use this to examine the association between current and previous values in a time series. Autocorrelation coefficients are plotted as a function of time-lag n and can be used to quantify the nature of autoregressive linkage in the time series (Fritts 1976), to estimate the decorrelation length needed to compute significances (see above), and to investigate oscillating patterns in time series.

Spectral analysis is a more powerful way than autocorrelation function analysis to describe cyclicity in time series by examining the strength of a periodic signal (*i.e.* the spectral power) in time series at different time frequencies (Jenkins and Watts 1968). It is worth noting that, in contrast to the autocorrelation, there are many different definitions of the spectrum. The evolution over time of the periodic signal can be analyzed using wavelet analysis (Torrence and Compo 1998). Performing a spectral analysis in CE results in a periodogram or spectrum in which the spectral power of the time series is plotted per cycle length (or 1/frequency) and significance levels of the spectral power based on Monte Carlo permutation tests are provided (Figure 4A). When producing a periodogram in CE, which is a simple Fourier transform of the input data, the spectral information from neighboring frequencies (and thus cycle lengths) can be averaged into bins, a simple boxcar spectrum. This reduces the number of frequency bins, but also the uncertainty inherent to each bin. The optimal number of bins to average over is therefore a trade-off between the error bars on the vertical (spectral power) and horizontal (frequency) axes of the spectrum. More sophisticated filtering options are not yet available.

The raw data for this periodogram or spectrum are available in column format, including the frequency in the first column, the spectral power in the second column, the power of a first-order autoregression (AR(1)) process fitted to the lag-1 autocorrelation (used for significance level calculations) in the third, and the significance level (*p*-value) in the fourth column. If there are more peaks in the spectrum above red-noise AR(1) process than expected by chance, the location of these is noted in text above the plot. Figure 4A shows the spectrum for JAF: we averaged frequencies into 10-frequency bins, which resulted

in 49 (rather than the original 490) frequency bins. JAF contains statistically significant cyclicity with cycles of approximately 2.5, 4 ($p < 0.01$), and 12 ($p < 0.05$) years in length.

A wavelet analysis (Figure 4B) shows that the 2-to-5 year cyclicity is fairly constant over time, whereas 10–20 year cycles are only prominent prior to A.D. 1500 and in the 20th Century. Running a wavelet analysis in CE thus results in a plot of the periodicity of the time series over time, with the strength (and significance level) of the spectral power represented by shading and a black line indicating the cone of influence. CE provides the option to select different types (Morlet, Paul, or DOG) and orders of wavelet functions, but for the purpose of paleoclimatology, this selection will have little influence on the resulting wavelet transform. Again, be aware that on average 10% of the area of the plot will appear significant at $p < 0.1$ even in the absence of any physical signal.

CONCLUSIONS

In this note, we provide a general introduction to the use of CE for high-resolution paleoclimatology. We describe a number of options for the exploration of instrumental data sets, and for the climatic and spatiotemporal analysis of user-defined paleoclimatic time series. It is worth noting, however, that the described options do not constitute the full spectrum of options available in CE and that CE is a dynamic operation that is regularly updated with new data sets and analysis tools. We therefore encourage researchers to further explore methods for engaging the CE tool in answering research-specific questions. Possible CE applications that are not explicitly covered in this paper and that could be further explored include the analysis of event-based (not normally distributed) time series and of lower-frequency (non-annual) time series and the comparison of paleoclimate time series with modeling simulations. Plans exist to link CE to the NOAA Paleoclimatology Website (http://www.ncdc.noaa.gov/paleo/data.html), which includes the International Tree-Ring Database (ITRDB). This collaboration will make a set of basic paleoclimatic research skills attainable for researchers from a wide range of disciplines.

A spectrum of index jafseas 1021:2001
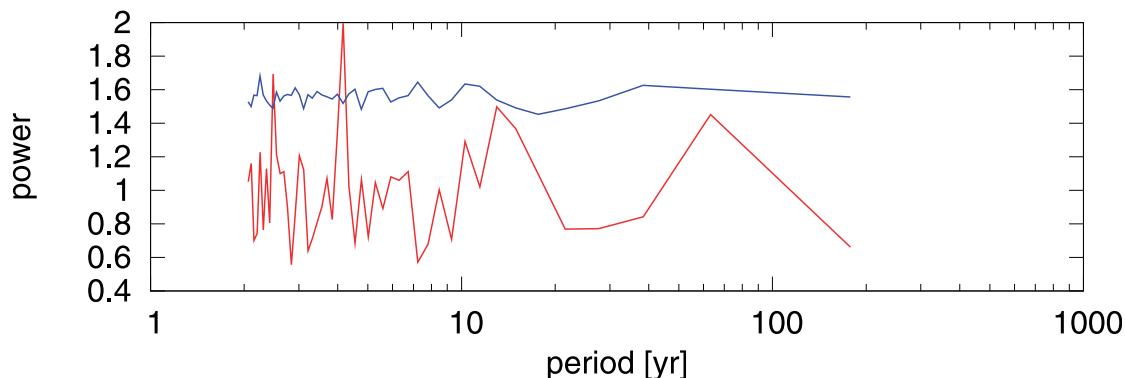
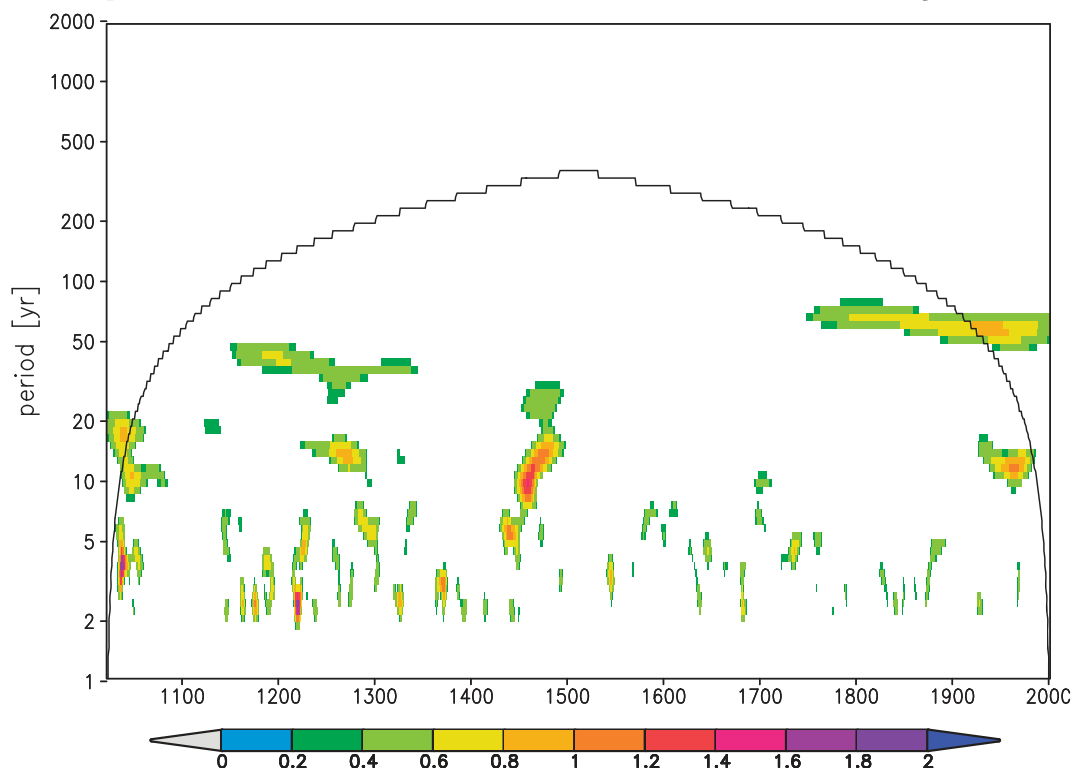## B power of Morlet 6 wavelet transform jafseas

Figure 4. Spectrum (10 period bins) (A) and morlet 6 wavelet transform (B) of the JAF tree-ring chronology (A.D. 1021–2001).

REFERENCES CITED

Abram, N. J., M. K. Gagan, J. E. Cole, W. S. Hantoro, and M. Mudelsee, 2008. Recent intensification of tropical climate variability in the Indian Ocean. *Nature Geosci* 1(12):849–853. http://www.nature.com/ngeo/journal/v1/n12/suppinfo/ngeo357_S1.html.

Baker, A., R. Wilson, I. J. Fairchild, J. Franke, C. Spotl, D. Mattey, V. Trouet, and L. Fuller, 2011. High resolution $\delta^{18}O$ and $\delta^{13}C$ records from an annually laminated Scottish stalagmite and relationship with last millennium climate. *Global and Planetary Change* 79(3–4):303–311. 10.1016/j.gloplacha.2010.12.007.

Briffa, K. R., T. J. Osborn, F. H. Schweingruber, P. D. Jones, S. G. Shiyatov, and E. A. Vaganov, 2002. Tree-ring width

and density data around the Northern Hemisphere: Part 1, local and regional climate signals. *Holocene* 12(6):737–757. 10.1191/0959683602hl587rp.

Brohan, P., J. J. Kennedy, I. Harris, S. F. B. Tett, and P. D. Jones, 2006. Uncertainty estimates in regional and global observed temperature changes: A new data set from 1850. *Journal of Geophysical Research-Atmospheres* 111(D12). D12106. 10.1029/2005jd006548.

Bromwich, D. H., and R. L. Fogt, 2004. Strong trends in the skill of the ERA-40 and NCEP-NCAR reanalyses in the high and midlatitudes of the southern hemisphere, 1958–2001. *Journal of Climate* 17(23):4603–4619. 10.1175/3241.1.

Buckley, B. M., K. Palakit, K. Duangsathaporn, P. Sanguantham, and P. Prasomsin, 2007. Decadal scale droughts over northwestern Thailand over the past 448 years: Links to the tropical Pacific and Indian Ocean sectors. *Climate Dynamics* 29(1):63–71. 10.1007/s00382-007-0225-1.

Büntgen, U., J. Franke, D. Frank, R. Wilson, F. Gonzalez-Rouco, and J. Esper, 2010. Assessing the spatial signature of European climate reconstructions. *Climate Research* 41(2): 125–130. 10.3354/Cr00848.

Camuffo, D., C. Bertolin, M. Barriendos, F. Dominguez-Castro, C. Cocheo, S. Enzi, M. Sghedoni, A. della Valle, E. Garnier, M. J. Alcoforado, E. Xoplaki, J. Luterbacher, N. Diodato, M. Maugeri, M. F. Nunes, and R. Rodriguez, 2010. 500-year temperature reconstruction in the Mediterranean Basin by means of documentary data and instrumental observations. *Climatic Change* 101(1–2):169–199. 10.1007/s10584-010-9815-8.

Compo, G. P., J. S. Whitaker, P. D. Sardeshmukh, N. Matsui, R. J. Allan, X. Yin, B. E. Gleason, R. S. Vose, G. Rutledge, P. Bessemoulin, S. Bronnimann, M. Brunet, R. I. Crouthamel, A. N. Grant, P. Y. Groisman, P. D. Jones, M. C. Kruk, A. C. Kruger, G. J. Marshall, M. Maugeri, H. Y. Mok, O. Nordli, T. F. Ross, R. M. Trigo, X. L. Wang, S. D. Woodruff, and S. J. Worley, 2011. The Twentieth Century Reanalysis Project. *Quarterly Journal of the Royal Meteorological Society* 137(654):1–28. 10.1002/qj.776.

Cook, E. R., 1985. *A Time-Series Analysis Approach to Tree-Ring Standardization*. Ph.D. dissertation, University of Arizona, Tucson; 171 pp.

Cook, E. R., C. A. Woodhouse, C. M. Eakin, D. M. Meko, and D. W. Stahle, 2004. Long-term aridity changes in the western United States. *Science* 306(5698):1015–1018. 10.1126/science.1102586.

Cook, E. R., K. J. Anchukaitis, B. M. Buckley, R. D. D'Arrigo, G. C. Jacoby, and W. E. Wright, 2010. Asian Monsoon failure and megadrought during the last millennium. *Science* 328(5977):486–489. 10.1126/science.1185188.

D'Arrigo, R., P. Baker, J. Palmer, K. Anchukaitis, and G. Cook, 2008. Experimental reconstruction of monsoon drought variability for Australasia using tree rings and corals. *Geophysical Research Letters* 35(12):L12709. 10.1029/2008gl034393.

D'Arrigo, R., N. Abram, C. Ummenhofer, J. Palmer, and M. Mudelsee, 2011. Reconstructed streamflow for Citarum River, Java, Indonesia: Linkages to tropical climate dynamics. *Climate Dynamics* 36(3–4):451–462. 10.1007/s00382-009-0717-2.

Diamond, H. J., and C. J. Lief, 2009. A comprehensive data portal for global climate information. *EOS, Transactions American Geophysical Union* 90(39):341. 10.1029/2009EO390001.

Efron, B., and R. Tibshirani, 1998. The problem of regions. *Annals of Statistics* 26(5):1687–1718.

Esper, J., D. Frank, U. Büntgen, A. Verstege, J. Luterbacher, and E. Xoplaki, 2007. Long-term drought severity variations in Morocco. *Geophysical Research Letters* 34(17):L17702. 17710.11029/12007gl030844.

Fan, Z. X., A. Brauning, B. Yang, and K. F. Cao, 2009. Tree ring density-based summer temperature reconstruction for the central Hengduan Mountains in southern China. *Global and Planetary Change* 65(1–2):1–11. 10.1016/j.gloplacha.2008.10.001.

Fritts, H. C., 1976. *Tree Rings and Climate*. Academic Press, London; 567 pp.

Gershunov, A., N. Schneider, and T. Barnett, 2001. Low-frequency modulation of the ENSO-Indian Monsoon rainfall relationship: Signal or noise? *Journal of Climate* 14:2486–2492. 10.1175/1520-0442(2001)014<2486:LFMOTE>2.0.CO;2.

Hansen, J., D. Johnson, A. Lacis, S. Lebedeff, P. Lee, D. Rind, and G. Russell, 1981. Climate impact of increasing atmospheric carbon-dioxide. *Science* 213(4511):957–966. 10.1126/science.213.4511.957.

Hansen, J., and S. Lebedeff, 1987. Global trends of measured surface air-temperature. *Journal of Geophysical Research-Atmospheres* 92(D11):13345–13372. 10.1029/JD092iD11p13345.

Hansen, J., R. Ruedy, M. Sato, and K. Lo, 2010. Global surface temperature change. *Reviews of Geophysics* 48:Rg4004. 10.1029/2010rg000345.

Harnik, N., and E. K. M. Chang, 2003. Storm track variations as seen in radiosonde observations and reanalysis data. *Journal of Climate* 16(3):480–495. 10.1175/1520-0442(2003)016<0480:stvasi>2.0.co;2.

Jenkins, G. M., and D. G. Watts, 1968. *Spectral Analysis and Its Applications*. Holden-Day, San Francisco; 541 pp.

Jones, P. D., 1994. Hemispheric surface air-temperature variations - a reanalysis and an update to 1993. *Journal of Climate* 7(11):1794–1802. 10.1175/1520-0442(1994)007<1794:hsatva>2.0.co;2.

Jones, P. D., and A. Moberg, 2003. Hemispheric and large-scale surface air temperature variations: An extensive revision and an update to 2001. *Journal of Climate* 16(2):206–223. 10.1175/1520-0442(2003)016<0206:halssa>2.0.co;2.

Kalnay, E., M. Kanamitsu, R. Kistler, W. Collins, D. Deaven, L. Gandin, M. Iredell, S. Saha, G. White, J. Woollen, Y. Zhu, M. Chelliah, W. Ebisuzaki, W. Higgins, J. Janowiak, K. C. Mo, C. Ropelewski, J. Wang, A. Leetmaa, R. Reynolds, R. Jenne, and D. Joseph, 1996. The NCEP/NCAR 40-year reanalysis project. *Bulletin of the American Meteorological Society* 77(3):437–471.

Kistler, R., E. Kalnay, W. Collins, S. Saha, G. White, J. Woollen, M. Chelliah, W. Ebisuzaki, M. Kanamitsu, V. Kousky, H. van den Dool, R. Jenne, and M. Fiorino, 2001. The NCEP-NCAR 50-year reanalysis: Monthly means CD-ROM and documentation. *Bulletin of the American Meteorological Society* 82(2): 247–267. 10.1175/1520-0477(2001)082<0247:tnnyrm>2.3.co;2.

Kuttel, M., E. Xoplaki, D. Gallego, J. Luterbacher, R. Garcia-Herrera, R. Allan, M. Barriendos, P. Jones, D. Wheeler, and

H. Wanner, 2010. The importance of ship log data: Reconstructing North Atlantic, European and Mediterranean sea level pressure fields back to 1750. *Climate Dynamics* 34(7–8):1115–1128. 10.1007/s00382-009-0577-9.

Luterbacher, J., E. Xoplaki, D. Dietrich, R. Rickli, J. Jacobeit, C. Beck, D. Gyalistras, C. Schmutz, and H. Wanner, 2002. Reconstruction of sea level pressure fields over the Eastern North Atlantic and Europe back to 1500. *Climate Dynamics* 18(7):545–561.

Luterbacher, J., D. Dietrich, E. Xoplaki, M. Grosjean, and H. Wanner, 2004. European seasonal and annual temperature variability, trends, and extremes since 1500. *Science* 303(5663):1499–1503.

Mitchell, T. D., and P. D. Jones, 2005. An improved method of constructing a database of monthly climate observations and associated high-resolution grids. *International Journal of Climatology* 25(6):693–712. 10.1002/joc.1181.

Morice, C. P., J. J. Kennedy, N. A. Rayner, and P. D. Jones, 2012. Quantifying uncertainties in global and regional temperature change using an ensemble of observational estimates: The HadCRUT4 data set. *Journal of Geophysical Research-Atmospheres* 117:D08101. 10.1029/2011jd017187.

Palmer, W. C., 1965. *Meteorological Drought*. Research paper, U.S. Dept. of Commerce, Washington; 58 pp.

Pauling, A., J. Luterbacher, C. Casty, and H. Wanner, 2006. Five hundred years of gridded high-resolution precipitation reconstructions over Europe and the connection to large-scale circulation. *Climate Dynamics* 26(4):387–405. 10.1007/s00382-005-0090-8.

Pederson, G. T., S. T. Gray, C. A. Woodhouse, J. L. Betancourt, D. B. Fagre, J. S. Littell, E. Watson, B. H. Luckman, and L. J. Graumlich, 2011. The unusual nature of recent snowpack declines in the North American Cordillera. *Science* 333(6040):332–335. 10.1126/science.1201570.

Poljansek, S., D. Ballian, T. A. Nagel, and T. Levanic, 2012. A 435-year long European black pine (*Pinus nigra*) chronology for the central-western Balkan region. *Tree-Ring Research* 68(1):31–44.

Press, W. H., S. A. Teukolsky, W. T. Vetterling, and B. P. Flannery, 1992. *Numerical Recipes in FORTRAN: The Art of Scientific Computing*. Cambridge University Press, New York; 963 pp.

Sturaro, G., 2003. A closer look at the climatological discontinuities present in the NCEP/NCAR reanalysis temperature due to the introduction of satellite data. *Climate Dynamics* 21(3–4):309–316. 10.1007/s00382-003-0334-4.

Torrence, C., and G. P. Compo, 1998. A practical guide to wavelet analysis. *Bulletin of the American Meteorological Society* 79(1):61–78.

Treydte, K., D. Frank, J. Esper, L. Andreu, Z. Bednarz, F. Berninger, T. Boettger, C. M. D'Alessandro, N. Etien, M. Filot, M. Grabner, M. T. Guillemin, E. Gutierrez, M. Haupt, G. Helle, E. Hilasvuori, H. Jungner, M. Kalela-Brundin, M. Krapiec, M. Leuenberger, N. J. Loader, V. Masson-Delmotte, A. Pazdur, S. Pawelczyk, M. Pierre, O. Planells, R. Pukiene, C. E. Reynolds-Henne, K. T. Rinne, A. Saracino, M. Saurer, E. Sonninen, M. Stievenard, V. R. Switsur, M. Szczepanek, E. Szychowska-Krapiec, L. Todaro, J. S. Waterhouse, M. Weigl, and G. H. Schleser, 2007. Signal strength and climate calibration of a European tree-ring isotope network. *Geophysical Research Letters* 34(24):L24302. 10.1029/2007gl031106.

Trouet, V., J. Esper, N. E. Graham, A. Baker, J. D. Scourse, and D. C. Frank, 2009. Persistent positive North Atlantic Oscillation mode dominated the Medieval Climate Anomaly. *Science* 324(5923). 10.1126/science.1166349.

Trouet, V., and A. H. Taylor, 2010. Multi-century variability in the Pacific North American circulation pattern reconstructed from tree rings. *Climate Dynamics* 35(6):953–963. 10.1007/S00382-009-0605-9.

Trouet, V., A. H. Taylor, E. R. Wahl, C. N. Skinner, and S. L. Stephens, 2010. Fire-climate interactions in the American West since 1400 CE. *Geophysical Research Letters* 37:L04702. 04710.01029/02009gl041695. L04702 10.1029/2009gl041695.

Trouet, V., M. Panayotov, A. Ivanova, and D. Frank, 2012. A Pan-European summer teleconnection mode recorded by a new temperature reconstruction from the eastern Mediterranean (1768–2008). *The Holocene*. DOI: 10.1177/0959683611434225.

van Oldenborgh, G. J., and G. Burgers, 2005. Searching for decadal variations in ENSO precipitation teleconnections. *Geophysical Research Letters* 32(15):L15701. 15710.11029/12005gl023110.

van Oldenborgh, G. J., S. Drijfhout, A. van Ulden, R. Haarsma, A. Sterl, C. Severijns, W. Hazeleger, and H. Dijkstra, 2009. Western Europe is warming much faster than expected. *Climate of the Past* 5(1):1–12.

Woodhouse, C. A., S. T. Gray, and D. M. Meko, 2006. Updated streamflow reconstructions for the Upper Colorado River Basin. *Water Resources Research* 42(5):W05415. W05415.

Xoplaki, E., J. Luterbacher, H. Paeth, D. Dietrich, N. Steiner, M. Grosjean, and H. Wanner, 2005. European spring and autumn temperature variability and change of extremes over the last half millennium. *Geophysical Research Letters* 32(15): L15713. 10.1029/2005gl023424.

Young, G. H. F., D. McCarroll, N. J. Loader, and A. J. Kirchhefer, 2010. A 500-year record of summer near-ground solar radiation from tree-ring stable carbon isotopes. *Holocene* 20(3):315–324. 10.1177/0959683609351902.